CLOUDLESS ATMOSPHERES FOR L/T DWARFS AND EXTRA-SOLAR GIANT PLANETS

P. Tremblin[1,2] and D. S. Amundsen[1,3,4] and G. Chabrier[1,5] and I. Baraffe[1,5] and B. Drummond[1] and S. Hinkley[1] and P. Mourier[5,6] and O. Venot[7]

Draft version January 15, 2016

ABSTRACT

The admitted, conventional scenario to explain the complex spectral evolution of brown dwarfs (BD) since their first detections twenty years ago, has always been the key role played by micron-size condensates, called "dust" or "clouds", in their atmosphere. This scenario, however, faces major problems, in particular the J-band brightening and the resurgence of FeH absorption at the L to T transition, and a physical first-principle understanding of this transition is lacking. In this paper, we propose a new, completely different explanation for BD and extrasolar giant planet (EGP) spectral evolution, without the need to invoke clouds. We show that, due to the slowness of the CO/CH_4 and N_2/NH_3 chemical reactions, brown dwarf (L and T, respectively) and EGP atmospheres are subject to a thermo-chemical instability similar in nature to the fingering or chemical convective instability present in Earth oceans and at the Earth core/mantle boundary. The induced small-scale turbulent energy transport reduces the temperature gradient in the atmosphere, explaining the observed increase in near infrared J - H and J - K colors of L dwarfs and hot EGPs, while a warming up of the deep atmosphere along the L to T transition, as the CO/CH_4 instability vanishes, naturally solves the two aforementioned puzzles, and provides a physical explanation of the L to T transition. This new picture leads to a drastic revision of our understanding of BD and EGP atmospheres and their evolution.

Subject headings: Methods: observational — Methods: numerical — brown dwarfs — planets and satellites: atmospheres

1. INTRODUCTION

The role of clouds in brown dwarf (BD) and extra-solar giant planet (EGP) atmospheres has been an intense subject of research for the past twenty years, since the first observations of these objects (e.g. Tsuji et al. 1996; Allard et al. 2001; Ackerman and Marley 2001; Burrows et al. 2006; Marley et al. 2010; Morley et al. 2014). While cloudy atmosphere models reproduce the observed reddening in infrared (IR) J - H and J - K colors (Burrows et al. 2006; Saumon and Marley 2008; Allard et al. 2001), several problems remain unsolved:

- The driving mechanism of the cloud dynamics remains poorly understood. Although convective overshooting has been proposed for such a mechanism (Freytag et al. 2010), the low variability of L dwarfs (Metchev et al. 2015, and references therein), which points to a relatively steady process, seems incompatible with the transient nature of overshooting. Furthermore, the change of regime in this mechanism and the sharpness in effective temperature of the LT transition, so in short the very physical nature of this transition remain so far unexplained.

tremblin@astro.ex.ac.uk or pascal.tremblin@cea.fr
[1] Astrophysics Group, University of Exeter, EX4 4QL Exeter, UK
[2] Maison de la Simulation, CEA-CNRS-INRIA-UPS-UVSQ, USR 3441, Centre d'étude de Saclay, 91191 Gif-Sur-Yvette, France
[3] Department of Applied Physics and Applied Mathematics, Columbia University, New York, NY 10025, USA
[4] NASA Goddard Institute for Space Studies, New York, NY 10025, USA
[5] Ecole Normale Supérieure de Lyon, CRAL, UMR CNRS 5574, 69364 Lyon Cedex 07, France
[6] Département de Physique, Ecole Normale Supérieure, 24 Rue Lhomond, F-75005 Paris, France
[7] Instituut voor Sterrenkunde, Katholieke Universiteit Leuven, Celestijnenlaan 200D, 3001 Leuven, Belgium

- Neither the J band brightening nor the FeH resurgence at the L/T transition are understood. Although holes in the cloud cover can reproduce these features (Ackerman and Marley 2001; Burgasser et al. 2002; Marley et al. 2010), Buenzli et al. (2015) recently showed that the variability of the spectrum is not compatible with holes but rather with height variations. The conclusion of Buenzli et al. (2015) is indeed that the explanation for the re-emergence of FeH still remains to be found.

- The absorption feature at 10 μm is not well reproduced with the current cloud models. Although some observations do suggest the presence of silicate dust (Cushing et al. 2006), the absorption feature is not present in all observed spectra and, for the ones that display it (e.g. 2M224, 2M0036, 2M1507, and 2M2244 in Stephens et al. 2009), cloud models cannot reproduce *both* the NIR reddening and the 10-μm absorption.

- Signatures of cloud polarization expected from cloud models remain undetected (Goldman et al. 2009). Even though L dwarfs might not rotate fast enough nor have low enough surface gravity to be sufficiently oblate to produce detectable polarization (Sengupta and Marley 2010), this lack of detection questions the cloud hypothesis.

In Tremblin et al. (2015), we showed that the spectra and near-IR colors of T and Y dwarfs can be reproduced without clouds if (i) non-equilibrium chemistry of NH_3 is taken into account, and (ii) the temperature gradient in the atmospheres of T dwarfs is reduced. In this paper, we explore a similar mechanism for L dwarfs and hot EGPs, using Denis-P 0255 and HR8799c, respectively, as typical templates, and show that these effects adequately reproduce both the FeH resurgence and the J-band brightening at the L/T transition.

We show that a physical process responsible for the temperature gradient reduction in L and T dwarf atmospheres is the chemical or (compositional) convection triggered by a thermo-chemical instability at the CO/CH_4 and N_2/NH_3 transitions. Finally, we discuss the implications and the limitations of this scenario.

2. SPECTRAL MODELS FOR HR8799C AND DENIS-P 0255

We use the same setup as described in Tremblin et al. (2015) i.e., a 1D spectral code ATMO with correlated-k coefficients for the radiative transfer, developed and tested in Amundsen et al. (2014), coupled to the CHNO-based chemical network of Venot et al. (2012). We improved our chemical and opacity database with the inclusion of the FeH molecule and used Wende et al. (2010) for the line list, Sharp and Burrows (2007) broadening coefficients, and Visscher et al. (2010) for the chemical equilibrium of FeH. In Tremblin et al. (2015), we applied the calculations to T dwarfs and showed that a reduced temperature gradient in the atmosphere, as reproduced with an effective adiabatic index ($\gamma \sim 1.2$ - 1.3) lower than the equilibrium value ($\gamma \sim 1.3$ - 1.4) correctly reproduces the observed spectra and the reddening in J - H colors, yielding a synthetic spectrum similar to the one with the inclusion of clouds (Morley et al. 2012). We have explored these effects on the EGP HR8799c (Fig. 1) and the L dwarf Denis-P 0255 (Fig. 2). As seen in figures 1 and 2, the models reproduce the observed spectra very well provided that (i) we include non-equilibrium chemistry and quench CO/CH_4 (i.e. prevent the formation of CH_4), (ii) we decrease the adiabatic index to $\gamma \sim 1.05$ in the lower part of their atmospheres. The only difference with the T-dwarf modeling of Tremblin et al. (2015) is that we modify the adiabatic index only within the layers corresponding to the emerging flux bands. The global effect of the modification of the adiabatic index along the L sequence and the L/T transition is shown in Fig. 3, and the modified layers are indicated in the pressure/temperature (PT) profiles in Fig. 4.

The data for HR8799c are taken from Oppenheimer et al. (2013), Ingraham et al. (2014), and Skemer et al. (2014). In Fig. 1, the blue spectrum is the out-of-equilibrium model obtained with a value of the turbulent diffusion coefficient $K_{zz} = 10^{11}$ cm^{2}s^{-1}. Such a high value is consistent with the convective velocities computed in the model for these low gravities. The 3.78-μm flux is higher in our model, but PH_3 opacity could be significant around 4 μm and is not included in our models (see Morley et al. 2014). Our out-of-equilibrium cloudless model with a modified adiabatic index provides a better fit to the NIR data between 1 and 2 μm compared to the cloud models (Ingraham et al. 2014). The effective temperature, surface gravity and radius we derive are compatible with evolutionary models (Baraffe et al. 2003) and suggest a lower-mass, younger object (3 M_{Jup} at 10 M_{yrs}) than previous studies. Since we used a higher metallicity, however, different C/O ratios could also lead to a good fit with slightly different values of effective temperature, surface gravity and radius. These effects need to be investigated in more details in follow-up studies.

The spectrum of Denis-P 0255 was obtained from Cushing et al. (2005). This object is a typical late type L dwarf (L8) which has a characteristic reddening in J - H and J - K. The model we used includes a zone with a modified adiabatic index $\gamma = 1.05$ in the deep atmosphere. As a result, the atmospheric profile has cooler deep layers and hotter upper ones than the equilibrium atmosphere (see Fig. 4). As a conse-

quence, the fluxes in Y and J bands are reduced and the ones in H and K bands are enhanced. The modeled spectrum shows that this effect adequately reproduces the main characteristics of the data, provided CH_4 is still reduced compared to the equilibrium value (with now a value $K_{zz} = 10^{7.5}$ cm^{2}s^{-1}, consistent, again, with the convective velocities computed in the model for these gravities). The effect is similar to what was inferred in Tremblin et al. (2015) for T dwarfs at the N_2/NH_3 transition. L dwarfs just require a lower value of the adiabatic index in order to produce a stronger reddening.

3. L/T TRANSITION AND FEH RESURGENCE

From our T-dwarf modeling in Tremblin et al. (2015), it was unclear whether the need to use cooler deep atmospheric layers was due to a real effect (fingering convection) or was rather a way to mimic the effect of clouds. The left panel of Fig. 3 displays the evolution of the spectrum along the L sequence (from T_{eff} = 1600 K to 1400 K). As expected, we clearly see a weakening of the FeH spectral signature as a function of decreasing effective temperature. The right panel of Fig. 3 illustrates the evolution of the spectrum at constant T_{eff} (= 1400 K) along the L/T transition when varying the modified adiabatic index from a value $\gamma = 1.05$, for L dwarfs, to $\gamma = 1.2$-1.3, for early T dwarfs. Observations (Golimowski et al. 2004) indeed suggest that the L/T transition occurs at relatively constant effective temperature. Figure 3 clearly shows that along this transition our models naturally yield a resurgence of the FeH absorption feature and a brightening of the J band flux similar to what was found in observations.

The L dwarf reddening is due to cooler deep atmospheric layers than the ones corresponding to a radiatively stable atmosphere, a consequence, as detailed in the next section, of the enhanced energy transport due to local chemical turbulence, triggered by the thermo-chemical instability. As one moves towards cooler atmospheres when transitioning towards T dwarfs, the instability vanishes. Turbulent dissipation warms up the deep atmosphere, steepening the temperature gradient (yielding a larger effective adiabatic index), increasing the FeH abundance and the flux in these hotter layers, compared to the L-dwarf profile. This global effect is illustrated in Fig. 4 . Along the L sequence, the atmospheric profiles keep cooling down, notably in the deeper layers ($P \geq 1$ bar), due to the smaller thermal gradient (i.e. the smaller effective adiabatic index). Along the L/T transition, the deep layers warm up, yielding a steeper temperature gradient, while the upper layers keep cooling down. An alternative suggested scenario to explain the resurgence of FeH and the J band brightening is holes in the cloud cover (Ackerman and Marley 2001; Burgasser et al. 2002; Marley et al. 2010) although it appears to be partly excluded by Buenzli et al. (2015). We rather suggest that the proper explanation for these puzzling spectral behaviors is (i) cooler deep atmospheres for L dwarfs than obtained with cloudy atmospheres, the conventional explanation for the past 20 years, yielding the J - H and J - K reddening, and (ii) a warming up of the deep layers at the L-T transition, due to small-scale turbulent dissipation, which explains both the FeH resurgence and the J band brightening.

4. INSTABILITY OF THE CO/CH_4 AND N_2/NH_3 TRANSITION

Although we have a model that can reproduce all the observed effects, we need an explanation for the change in the modified adiabatic index and the transition from $\gamma = 1.05$ to 1.2-1.3. In Tremblin et al. (2015), we proposed that
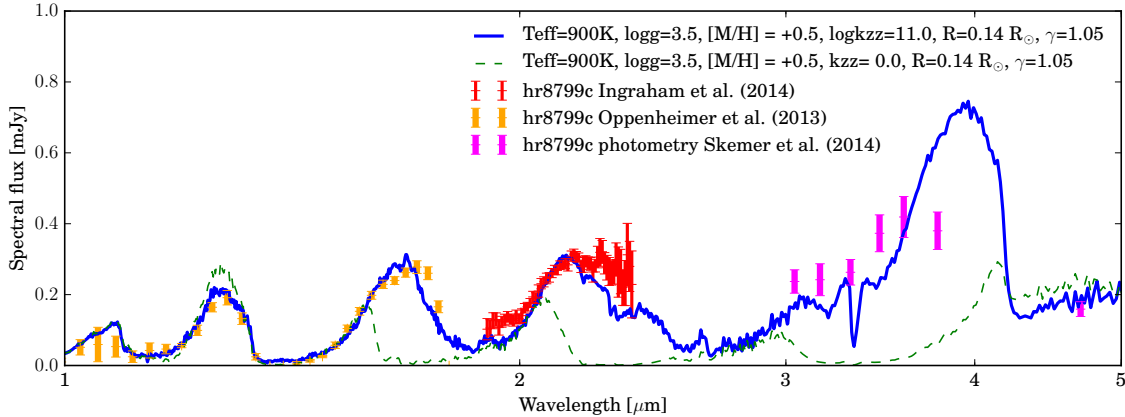
Figure 1. Spectral modeling of HR8799c. The blue spectrum is a model with out-of-equilibrium chemistry with $K_{zz} = 10^{11}$ cm^{2}s^{-1}. The green dashed model shows the corresponding equilibrium model with the same PT structure in order to illustrate the effect of the change in the CH$_4$ abundance profile.
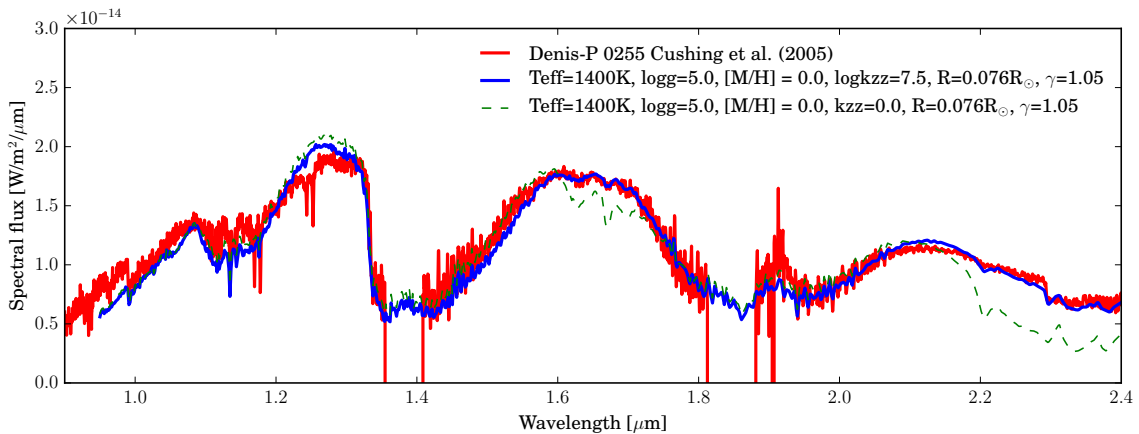
Figure 2. Spectral modeling of the L8 dwarf Denis-P 0255. The blue model is a model with out-of-equilibrium chemistry with $K_{zz} = 10^{7.5}$ cm^{2}s^{-1}. The green dashed model shows the corresponding equilibrium model with the same PT structure in order to illustrate the effect of the change in the CH$_4$ abundance profile.

small scale "diffusive" turbulence, more efficient than radiative transport, induced by fingering convection triggered by thin dust condensation, would be responsible for the decrease of the temperature gradient. We revisit this scenario and rather suggest that the real culprit is the instability of carbon and nitrogen chemistry in BD and EGP atmospheres. Within the temperature range of interest, carbon is preferentially in form of CO at high temperature and of CH$_4$ at low temperature. Similarly, nitrogen changes from N$_2$ at high temperature to NH$_3$ at low temperature. The net reactions for these transitions are:

$$CO + 3H_2 \rightarrow CH_4 + H_2O$$
$$N_2 + 3H_2 \rightarrow 2NH_3 \qquad (1)$$
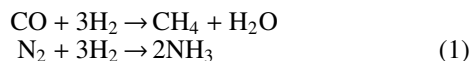
It is quite clear that the part of the atmosphere in the methane or ammonia dominant state will have a higher mean molecular weight than the corresponding CO or N$_2$ dominated one, since there are globally fewer molecules in these latter states. On the other hand, it is well known from chemical network studies that the chemistry for these transitions can be very slow (Venot et al. 2012; Moses et al. 2011). Therefore, atmospheres with these chemical transitions can develop an instability similar in nature to fingering double diffusive convection, but with the chemical reactions themselves now playing the role played otherwise by molecular diffusion, leading to a

thermo-chemical instability. The analogy is as follows: at the CH$_4$/CO transition, if a perturbation drives some "CH$_4$+H$_2$O" mixture down in the "CO+3H$_2$" (warmer) deeper layers, and if we are in the stable radiative part of the atmosphere, because of the slowness of the chemical reaction the mixture will stay in its methane-rich state and sink because of its higher molecular weight. The same process can happen at the N$_2$/NH$_3$ transition. The extent of the unstable zone can be estimated by using an extension of the Ledoux criterion (Rosenblum et al. 2011):

$$R_0 = \frac{\nabla_T - \nabla_{\rm ad}}{\nabla_\mu} < \frac{1}{\tau} = \frac{\kappa_T}{l^2/\tau_{\rm chem}} \qquad (2)$$

We have replaced the usual molecular diffusion coefficient by $l^2/\tau_{\rm chem}$ with $\tau_{\rm chem}$ the timescale of the chemical reaction and l the typical size of the unstable structures. We have computed the timescales for the reactions using the equations given by Zahnle and Marley (2014), and we assumed that the typical size of the unstable structures is 1% of the scale height (see Traxler et al. 2011, for a discussion on the size of the fingers expected in the stellar context). In order to be conservative, we use an upper limit for R_0, given by $R_{\rm max} = \nabla_{\rm ad}/|\nabla_\mu|$. The unstable regions are portrayed in the top panel of Fig. 5 for the CO/CH$_4$ chemistry in an L dwarf at T$_{\rm eff}$ = 1400 K and for the N$_2$/NH$_3$ chemistry for a T dwarf at T$_{\rm eff}$ = 600 K. For
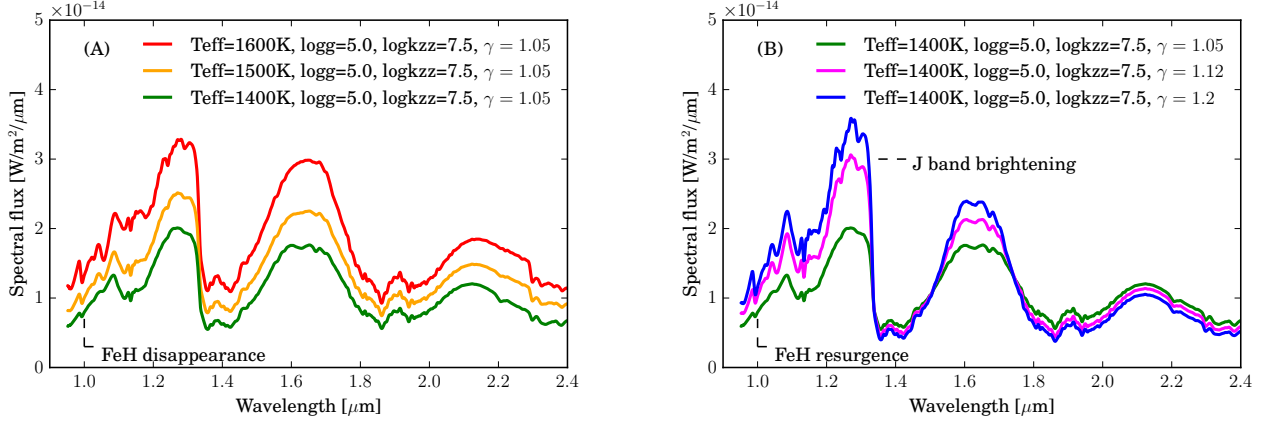
Figure 3. Left: spectral sequence along L dwarfs showing the disappearance of FeH with lower effective temperature. Right: spectral sequence along the L/T transition at constant effective temperature, showing the resurgence of FeH and the brightening of the J band.
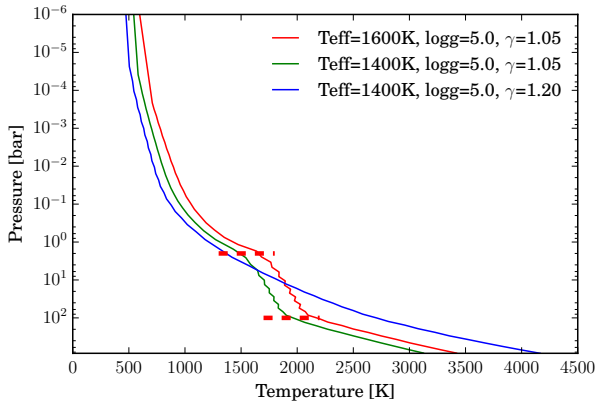
Figure 4. Pressure/Temperature structures of our models along the L sequence (T_{eff}=1600K to T_{eff}=1400K) and along the L/T transition at constant effective temperature (γ=1.05 to γ=1.2).

simplicity we derived the mean-molecular-weight gradient ∇_μ from the difference between a full ammonia or methane state and a full CO or N_2 state over one scale height H, reduced by a factor l/H (i.e. $\nabla_\mu \sim -10^{-5}$ for CO/CH$_4$ and $\nabla_\mu \sim -10^{-6}$ for N_2/NH$_3$). The left panel of Fig. 5 shows that the chemical transitions in all the upper atmosphere of a L or T dwarf are unstable, because of the slow chemistry. In the bottom panel of Fig. 5, we compare the color magnitude diagram (CMD) M_J versus J - H obtained with the equilibrium models and with the models with out-of-equilibrium chemistry and a modified adiabatic index. As for the T dwarfs in Tremblin et al. (2015), the L-dwarf reddening is well reproduced in the CMD with the temperature-gradient reduction. Other CMDs with the NIR bands Y, J, H, and K give a similar good match between our models and the observations since, as shown in Fig. 2, the NIR spectra are well reproduced. We also illustrate the transition from L to T with a model at constant effective temperature and an adiabatic index varying from 1.05 (L) to 1.25 (T) (orange line in Fig. 5). This highlights the occurence of the J-band brightening in our (cloudless) 1D models, even though a detailed sequence based on consistent evolutionary models is needed to properly take into account the evolution of gravity, effective temperature and modified adiabatic index. This will be explored in a forthcoming paper. We indicate the domains where the CO/CH$_4$ and N_2/NH$_3$ transitions are predicted to be unstable. The sharpness of the limits correspond-

ing to the instability, according to the above modified Ledoux criterion, naturally explains the sharpness of the L/T transition. Indeed, as temperature decreases, reaching the later T dwarf regime, the CO/CH$_4$ transition will lie at deeper levels than the ones subject to the instability, so that the now CH$_4$-dominated atmosphere will become stable again, as the chemical reaction timescale τ_{chem} becomes shorter than the radiative timescale. This does not preclude, however, the presence of some (quenched) CH$_4$ in the upper layers of L dwarf atmospheres.

5. DISCUSSION AND CONCLUSIONS

In this paper, we show that:

- Conditions characteristic of the atmospheres of L dwarfs favor the onset of a thermo-chemical instability at the CO/CH$_4$ transition, while conditions typical of T dwarf atmospheres yield the same instability at the N_2/NH$_3$ transition. The instability is due to the development of a destabilizing molecular weight gradient induced by the slowness of these chemical equilibrium reactions. This gradient generates local chemical (compositional) convection, which decreases the temperature gradient in the atmosphere.

- The spectra of L dwarfs and hot EGPs is well reproduced if (i) the temperature gradient in the atmosphere is decreased, because of the aforementioned instability, and (ii) if the quenching of CH$_4$ at the CO/CH$_4$ transition is taken into account. The same picture applies to T dwarfs, with quenching of NH$_3$ at the N_2/NH$_3$ transition.

- As the instability vanishes along the L/T transition, small scale turbulent dissipation warms up the deep layers and thus increases the temperature gradient in the atmosphere. This naturally explains the so far unexplained FeH resurgence and J-band brightening in early T dwarfs.

A detailed numerical analysis of the instability is certainly needed to determine the growth rate and the size of the most unstable mode and thus the typical time and space scales of the instability. The efficiency of the induced small-scale turbulent energy transport and dissipation also need to be determined in order to properly quantify (i) the modified adiabatic
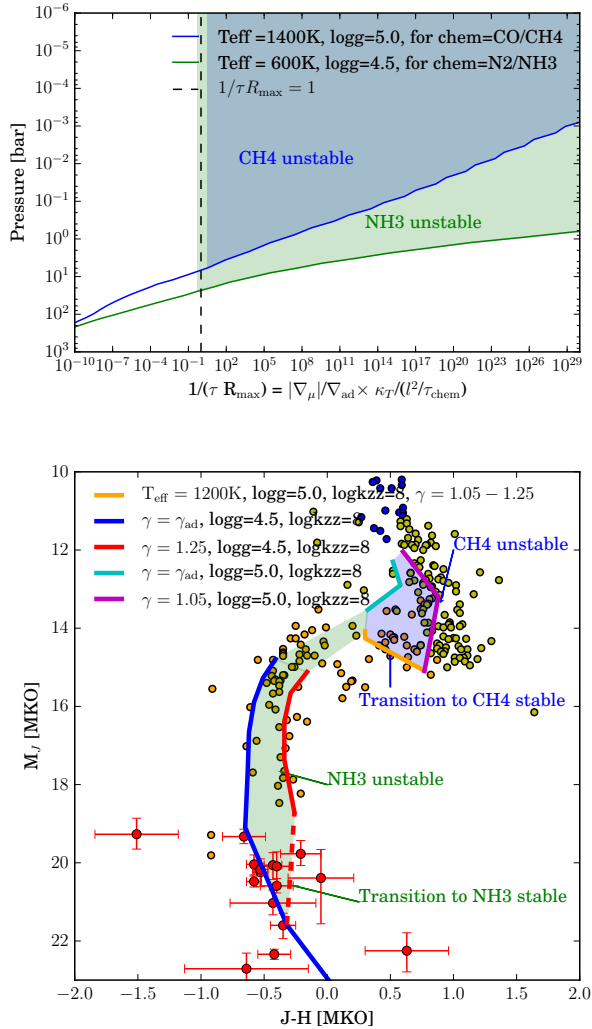
Figure 5. Top: Profiles of $1/(\tau\,R_{max})$ for a typical L dwarfs with a CO/CH$_4$ transition and for a typical T dwarf with a N$_2$/NH$_3$ transition. The part of the atmosphere unstable to the modified Ledoux criterion is indicated with the shaded colors. Bottom: M$_J$ versus $J - H$ color magnitude diagram for brown dwarfs compared to our equilibrium models (blue and cyan) and our out-of-equilibrium adiabatic-index-modified models (red and magenta). We also plot (as a guideline) the transition from L to T at a constant effective temperature of 1200 Kelvin (orange). We indicate the possible zone where the objects will be subject to the thermo-chemical instability if the CO/CH$_4$ transition and the N$_2$/NH$_3$ transition. The Y-dwarf photometry is from Dupuy and Kraus (2013); Beichman et al. (2014) and the L/T/M from Dupuy and Liu (2012); Faherty et al. (2012).

index, (ii) the amount of turbulent heating which yields an increase of temperature in the deep atmospheric layers at the L/T transition. Such studies require non-trivial numerical explorations.

Although by no means providing a proof, several features bring support to the reality of this instability. First, its disappearance when the atmosphere becomes stable again (according to condition 2) could explain the sharpness in effective temperature of the L/T transition. Second, turbulent energy transport, triggered by the instability of the CO/CH$_4$ and N$_2$/NH$_3$ transitions, decreases the temperature gradient in the atmosphere, leading to the reddening of L and T dwarfs, respectively. Third, the strength of the instability being intrinsically linked to the magnitude of the mean-molecular-weight

gradient, the fact that the gradient associated to the CO/CH$_4$ transition is larger than the one at the N$_2$/NH$_3$ transition (because of the C/N $\sim$ 4 abundance ratio Asplund et al. 2009) explains the stronger reddening for L dwarfs than for T dwarfs. Fourth, the turbulence induced by CO or temperature fluctuations in the atmosphere during the transition from CO to CH4 at the L/T transition could explain the observed variability. Thus the fluctuations observed by Doppler imaging reflect the ones in CO abundances or in temperature (Crossfield et al. 2014).

Given the coherence of this global picture, we conclude that clouds are not needed to explain the main characteristics of the emission spectra of BDs and directly imaged EGPs. We emphasize that this does not imply an absence of clouds. Given the possibility of many stable condensates, and the presence, according to the present scenario, of turbulent layers, these atmospheres very likely present some cloud cycles. Furthermore, some observations, such as the absorption in the 10 μm window (e.g. Cushing et al. 2006), suggest the presence of condensates. Current cloud models, however, do not well reproduce this signature (see Stephens et al. 2009), requiring a revision of the models in order to reproduce both this signature and the NIR color reddening.

Not only does the present scenario completely change our present understanding (and non understanding) of BD and EGP atmospheres, but, if correct, it shows that the same physical mechanism, namely chemical or fingering convection, induced by a thermo-chemical instability, would take place in environments as different as Earth oceans (Rahmstorf 2003), the Earth core-mantle boundary (Hansen and Yuen 1988), and exoplanet and brown dwarf atmospheres, nicely illustrating the universality of physical processes in nature.

REFERENCES

Ackerman, A. S. & Marley, M. S. 2001, ApJ, 556, 872
Allard, F., Hauschildt, P. H., Alexander, D. R., et al. 2001, ApJ, 556, 357
Amundsen, D. S., Baraffe, I., Tremblin, P., et al. 2014, A&A, 564, 59
Asplund, M., Grevesse, N., Sauval, A. J., et al. 2009, ARA&A, 47, 481
Baraffe, I., Chabrier, G., Barman, T. S., et al. 2003, A&A, 402, 701
Beichman, C., Gelino, C. R., Kirkpatrick, J. D., et al. 2014, ApJ, 783, 68
Buenzli, E., Marley, M. S., Apai, D., et al. 2015, ApJ, 812, 163
Burgasser, A. J., Marley, M. S., Ackerman, A. S., et al. 2002, ApJL, 571, L151
Burrows, A., Sudarsky, D., & Hubeny, I. 2006, ApJ, 640, 1063
Crossfield, I. J. M., Biller, B., Schlieder, J. E., et al. 2014, Nature, 505, 654
Cushing, M. C., Rayner, J. T., & Vacca, W. D. 2005, ApJ, 623, 1115
Cushing, M. C., Roelling, T. L., Marley, M. S., et al., 2006, ApJ, 648, 614
Dupuy, T. J., & Kraus, A. L. 2013, Science, 341, 1492
Dupuy, T. J., & Liu, M. C. 2012, ApJS, 201, 19
Faherty, J. K., Burgasser, A. J., Walter, F. M., et al. 2012, ApJ, 752, 56
Freytag, B., Allard, F., Ludwig, H. G., et al. 2010 A&A, 513, A19
Goldman, B., Pitann, J., Zapatero Osorio M. R., et al. 2009, A&A, 502, 929
Golimowski, D. A., Leggett, S. K., Marley, M. S., et al. 2004, AJ, 127, 3516
Hansen, U. & Yuen, D. A. 1988, Nature, 334, 237
Ingraham, P., Marley, M. S., Saumon, D., et al. 2014, ApJL, 794, L15

6

Marley, M. S., Saumon, D., & Goldblatt, C. 2010, ApJL, 723, L117
Metchev, S. A., Heinze, A., Apai, D., Flateau, D., et al. 2015, ApJ, 799, 154
Morley, C. V., Fortney, J. J., Marley, M. S., et al. 2012, ApJ, 756, 172
Morley, C. V., Marley, M. S., Fortney, J. J., et al. 2014, ApJ, 787, 78
Moses, J. I., Visscher, C., Fortney, J. J., et al. 2011, ApJ, 737, 15
Oppenheimer, B. R., Baranec, C., Beichman, C., et al., 2013, ApJ, 768, 24
Radigan, J. 2014, ApJ, 797, 120
Rahmstorf, S. 2003, Nature, 421, 699
Rosenblum, E., Garaud, P., Traxler, A., et al. 2011, ApJ, 731, 66
Saumon, D. & Marley, M. S. 2008, ApJ, 689, 1327
Sengupta, S. & Marley, M. S., 2010, 722, L142
Sharp, C. M. & Burrows, A. 2007, ApJS, 168, 140

Skemer, A. J., Marley, M. S., Hinz, P. M. 2014, ApJ, 792, 17
Stephens, D. C., Leggett, S. K., Cushing, M. C., et al., 2009, 702, 154
Traxler, A., Garaud, P., & Stellmach, S. 2011, ApJL, 728, L29
Tremblin, P., Amundsen, D. S., Mourier, P., et al. 2015, ApJL, 804, L17
Tsuji, T., Ohnaka, K., Aoki, W. 1996, A&A, 305, L1
Venot, O., Hébrard, E., Agúndez, M. 2012, A&A, 546, 43
Visscher, C., Lodders, K., & Fegley, B. J. 2010, ApJ, 716, 1060
Wende, S., Reiners, A., Seifahrt, A., et al. 2010, A&A, 523, A58
Zahnle, K. J. & Marley, M. S. 2014, ApJ, 797, 41